LOCAL SHELL-SIDE HEAT-TRANSFER COEFFICIENTS IN THE VICINITY OF SEGMENTAL BAFFLES IN TUBULAR HEAT EXCHANGERS

M. S. Gurushankariah, and J. G. Knudsen
Oregon State College, Corvallis, Oregon

Preprint 19

Presented at the

Second National Heat Transfer Conference

A.I.Ch.E.-A.S.M.E.

Chicago, Illinois

August 18 to 21, 1958

Preprinted for the conference by

AMERICAN INSTITUTE OF CHEMICAL ENGINEERS
25 West 45 Street, New York 36, New York

ABSTRACT

Local heat-transfer coefficients were studied in detail in the central baffle space between two segmental baffles in a tubular heat exchanger. Two baffle spacings and three flow rates were investigated. Average overall Nusselt numbers determined from the measured local coefficients compare favorably with average Nusselt numbers measured by other workers. The data are presented in picture form which enabled the drawing up of a schematic diagram of the flow pattern in the baffle space. The results indicate the presence of three flow zones between two baffles. The longitudinal-flow zone occurs in the baffle windows. The cross-flow zone and eddy-flow zone occur on the downstream and upstream sides of the baffle space respectively. Heat transfer rates were in general higher in the eddy-flow zone. The heat transfer rate varies along individual tubes from a maximum at the baffle to a minimum midway between the baffle. The minimum value is one-fourth to one-half the value at the baffle.

LOCAL SHELL-SIDE HEAT-TRANSFER COEFFICIENTS IN THE VICINITY OF SEGMENTAL BAFFLES IN TUBULAR EXCHANGERS

by

M. S. Gurushankariah*
J. G. Knudsen

Oregon State College
Corvallis, Oregon

Heat transfer is an important unit operation in industrial processes. It is common practice to transfer heat from one flowing fluid to another and for this purpose segmental baffled tubular heat exchangers are widely used. In these exchangers it is relatively easy to predict the heat-transfer coefficient for the fluid flowing in the tubes. However, flow on the shell-side of the tube is very complicated due to the complex baffling arrangement. For this reason prediction of shell-side heat-transfer coefficients is difficult.

There has been little fundamental study of heat transfer on the shell-side of baffled heat exchangers. Most workers have measured average coefficients over the whole exchanger and variation of the coefficient throughout the tube bundle due to baffle spacing, clearances, etc., was not determined. Gupta and Katz (4) made visual studies of water flowing in a glass heat exchanger and detected three distinct flow zones; (1) a longitudinal-flow zone, (2) a cross-flow zone, (3) an eddy-flow zone. In addition, these workers provided relationships for predicting heat transfer rates in each flow zone. Ambrose and Knudsen (2) determined local shell-side heat-transfer coefficients in a segmental baffled exchanger and found wide variation of the coefficient

*Present address: Department of Chemical Engineering, Carnegie Institute of Technology, Pittsburgh, Pennsylvania

along the length of the bundle and around the individual tubes. These workers determined heat-transfer coefficients at the baffles and midway between the baffles. They were able to tentatively detect an eddy-flow zone and also showed the effect of baffle spacing and tube spacing on the heat-transfer coefficients. It appeared from this work that a detailed study of one baffle space was necessary in order to obtain more information on flow zones and heat-transfer rates in these zones.

The present work consists of a detailed study of the local shell-side heat-transfer coefficients in one baffle space in an exchanger. Two different baffle spacings were investigated. Local heat-transfer coefficients were determined around each tube in a fourteen-tube bundle at intervals of 3/4 of an inch between two segmental baffles. Three flow rates were studied for each baffle spacing.

Experimental Equipment

The major components of the experimental equipment consisted of a model heat exchanger, a sensing probe, a D-C power source, an emf metering arrangement and an air source. These components have been described in detail elsewhere (1), (2). The model shell-and-tube baffled heat exchanger had an effective length of 45 inches. A tube bundle of 14 one-inch OD aluminum condenser tubes was enclosed in a 6-inch diameter cast lucite plastic shell. A photograph of the apparatus is shown in Figure 1. Table I shows the exact dimensions of the parts.

The sensing probe could measure local temperatures at any point along or around any tube. It could also be readily moved from one tube location to the other. A photograph of the sensing probe is shown in Figure 2. Three one-inch wide by 0.002-inch thick pieces of Trophet C resistance ribbon having a resistance of 0.271 ohms/ft. and a thermal conductivity of 7.63 Btu/hr.

ft.^{2} ^oF/ft., were wrapped around the plastic bar as shown in Figure 2.

TABLE I

Dimensions of Heat Exchanger Components

Exchanger Shell				
Inside diameter	5.719	±	0.03	inches
Outside diameter	5.937	±	0.03	inches
Length	45.00			inches
Baffles				
Baffle diameter	5.594	±	0.002	inches
Height at Cut	4.290	±	0.002	inches
Drilled Holes	1.063	±	0.010	inches
Tubes				
Outside Diameter	1.000	±	0.001	inches
Drilled Holes				
Tube Holes in Tube Sheets	1.000	±	0.003	inches
Tie-Rod Holes	3/16			inch
Flange-Tube Sheet Bolt Holes	1/4			inch

The ribbons were held in position by copper bars which also supplied electric power. The power leads entered from the downstream side and the thermocouple wires entered from the upstream side through the plastic tube. The thermocouple junctions were located below the central ribbon and electrically insulated from it by "Saran Wrap". D-C power was supplied by passing A-C current through a Raytheon Voltage Stabilizer and a selenium rectifier. The emf developed in the thermocouples was measured with a Leeds and Northrup Precision potentiometer.

Experimental Data

Local shell-side heat-transfer coefficients were determined in detail in one baffle space for air flowing in a baffled tubular heat exchanger. Two baffle spacings of 6.43 inches and 4.09 inches and three flow rates of 60 cfm, 90 cfm and 120 cfm were investigated at three-quarter-inch intervals between the central two baffles. In all, about 5300 local heat transfer coefficients were determined*.

The data are presented in the manner shown in Figs. 3 and 4. Figure 3 shows the tube numbering system and is a guide to the data on Fig. 4. Figure 4 shows the results obtained for a baffle spacing of 4.05 in. (10 baffles in the exchanger) and for a flow rate of 90 cfm. The numbers in the segments are local heat-transfer coefficients except for the lower right segment which gives the average Nusselt number for the tube at that position. The shaded portions of the tubes represent the highest two or three measured coefficients. This shading helps to determine the direction of flow past the tube.

A summary of the experimental data is furnished in Table II. Data recorded were, the current in the resistance ribbon, millivolt readings from the seven sensing probe thermocouples and the air thermocouple, the pressure drop manometer reading, the orifice manometer reading, the pressures at the exchanger and the orifice, and the barometric pressure.

---

*Complete tabulated data are on file with the American Documentary Institute and may also be obtained from reference (4).

TABLE 2

Summary of Experimental Data

Tube Bundle - 14 one-inch OD tubes at 1-1/4 inch triangular pitch

Number of Baffles	Number of positions investigated along tubes	Total number of local coefficients measured	Air flow rate cfm ($60^{\circ}F$, 1 atm)
6	11	1078	58.65
6	11	1078	90.35
6	11	1078	119.30
10	7	686	58.73
10	7	686	90.38
10	7	686	117.60

Calculation of the local heat-transfer coefficient

A general expression for calculating the local heat-transfer coefficient is developed by making an energy balance around a differential length of resistance ribbon. The following equation results, as shown by Giedt (3)

$$h = \frac{\frac{i^2R}{W} + \frac{kZ}{r^2}\frac{d^2t}{d\theta^2} - \frac{q_{rad}}{A} - \frac{q_{cond}}{A}}{t - t_a} \qquad (1)$$

Like other investigators (1, 3) who used the resistance heating technique the radiation and conduction terms were assumed to be negligible. Neglecting these and substituting the numerical values of constants Eq. (1) becomes

$$h = \frac{11.10\ i^2 + 2404\ \frac{d^2t}{d\theta^2}}{t - t_a} \qquad (2)$$

This equation was used to calculate the local heat-transfer coefficients. The second derivative was evaluated using a Milne three-point method (6). The

actual calculation was performed on an Alwac IIIE digital computer. An average heat-transfer coefficient was evaluated at each position from the arithmetic average of the seven local coefficients around the circumference of the tube

$$h_{av} = \frac{1}{7} \sum_{i=1}^{i=7} h_i \qquad (3)$$

where h_i is the local coefficient measured on the surface of the tube. The average Nusselt number for each position was calculated using this average heat-transfer coefficient

$$Nu_{av} = \frac{h_{av} d}{k} \qquad (4)$$

Discussion of Results

1. Heat transfer rates along tubes

The average Nusselt numbers for each tube at each position investigated are shown in Fig. 5 for the 6 baffle case and a flow rate of 60 cfm. Positions 1 and 11 correspond to the baffle positions and high Nusselt numbers are found on all tubes at these points. There was 1/32-in. clearance between the tube and baffle. The Nusselt number at the baffle is not the same for each tube possibly indicating variation of flow rates through the baffle holes and eccentricity of the tube in the baffle hole.

Beyond the baffle the Nusselt number decreases rapidly and reaches a minimum value midway between the baffles. This minimum is one-fourth to one-half the value at the baffle hole.

In general the curve showing variation of Nusselt number with length is

nearly symmetrical between the baffles except for tubes 1, 10, 5, and 6. These are the tubes which pass through the baffle window and the minimum Nusselt number for these tubes occurs at a point about seven-tenths of the baffle space from the upstream baffle. For most other tubes the minimum Nusselt number occurs midway between the baffles.

Some of the curves shown in Fig. 5 have irregularities. These may be due to local areas of turbulence in the shell and they seem to occur mainly on tubes which are adjacent to the shell.

In Fig. 6 the average Nusselt number for all tubes at a given cross-section is plotted as a function of position along the length of the exchanger. This average Nusselt number Nu_c was obtained by averaging the average Nusselt number, Nu_{av} for each tube at a cross-section.

$$Nu_c = \frac{1}{14} \sum_{k=1}^{k=14} (Nu_{av})_k \qquad (5)$$

where $(Nu_{av})_k$ is the average Nusselt number for the k-th tube as determined by Eq. (4).

2. Correlation of Data

The data were correlated and compared with results obtained by other workers. To do this it was necessary to obtain the overall Nusselt number for the baffle space studied. This was done by determining the area under the curves in Fig. 6 and dividing by the baffle spacing, s, i.e.,

$$Nu_{oa} = \frac{1}{s} \int_0^s Nu_c ds \qquad (6)$$

where Nu_{oa} is the overall Nusselt number and includes each individual coefficient measured in the baffle space.

In Fig. 7 the quantity $Nu_{oa}\ Pr^{-1/3}$ is plotted versus the Reynolds number $d\ G_e/\mu$ where G_e is the weighted mass velocity determined from the free area at the baffle window and the free area of cross flow at the shell diameter.

$$G_e = \frac{W}{\sqrt{A_w\ A_c}} \tag{7}$$

The experimental results of Williams and Katz (7) and Ambrose and Knudsen (2) are included. The present data are well represented by line A which has a slope of 0.6. Reasonable agreement is obtained with that of other workers.

The results of Ambrose and Knudsen (2) were obtained on the same exchanger as the present data. The results of these workers are high because they investigated only 3 to 4 positions in a baffle space and therefore in the integration shown in Eq. (6) some error was involved in assuming a linear variation of the Nusselt number between the investigation positions. In the present work 7 to 11 positions were studied in the baffle space and the error involved by assuming linear variation between the positions is reduced.

Curve D of Fig. 7 shows the results of Williams and Katz (7) from a heat exchanger having the same tube diameter to pitch ratio as that studied in the present work. The present results are somewhat higher probably because of the clearance between the tube and baffle and because a larger tube was studied.

A comparison with the measurements of Ambrose (1) who used the same apparatus as the authors indicates a fair reproducibility of results for the common investigation positions. The comparison is shown in Fig. 8.

3. Effect of clearance between tube and baffle

In this work the baffle hole was 1/16-in. larger in diameter than the tube

thus providing a clearance of 1/32-in. between the tube and baffle. As shown in Figs. 5 and 6 high heat-transfer coefficients occur in the baffle holes. The actual effect of these high coefficients cannot be determined quantitatively until information is available on the amount of leakage which occurs in the clearances. When leakage occurs, the amount of fluid going around the baffle is decreased and therefore cross-flow heat-transfer coefficients are decreased. Whether this decrease is more than offset by the high coefficients in the baffle holes when clearances are present is not known.

4. Variation of heat transfer rates around tubes

It will be observed from Fig. 4 that for some tubes considerable circumferential variation of the local heat-transfer coefficient exists. The shaded portions of the tubes indicate the highest two or three values of the coefficient. When these highest values are considerably above the other coefficients on the circumference of the tube their position is taken to indicate the direction which the fluid is approaching tube at the particular position in question. This procedure is based on the fact that local coefficients in the vicinity of the forward stagnation point on an immersed cylinder are higher than at other points around the cylinder. For some tubes, there is small circumferential variation of the local coefficients. For these tubes and these positions, flow is assumed to be taking place parallel to the tube axis.

5. Pattern of flow in the baffle space

The variation of heat transfer coefficients around tubes is used as a basis for determining the pattern of flow in the baffle space as depicted in Fig. 9.

The flow patterns for each baffle spacing are essentially unchanged as the flow rate is increased from 60 to 120 cfm. The arrows in Fig. 9 indicate the direction which the fluid is approaching the tube. When a dot appears

motion perpendicular to the plane of the paper is indicated.

There is evidence that the shell-side flow is divided into three distinct zones; (1) the longitudinal-flow zone in the baffle window, (2) the cross-flow zone, (3) the eddy-flow zone. These results are in agreement with those of Gupta and Katz (4) and Ambrose and Knudsen(2). The cross-flow and eddy-flow zones divide the space between the baffles into approximately two equal parts. Considerable turbulence is detected particularly for the six baffle case as evidenced by flow perpendicular to the plane of the paper and reversal of flow between adjacent rows of tubes. The only clear cut pattern appears to be the cross-flow zone in the downstream half of the baffle space.

Average Nusselt numbers for each flow zone are plotted as a function of the flow rate in Fig. 10, and tabulated in Table 3. The longitudinal zone includes the space enclosed by the baffle window and a plane extending from the baffle cut of the upstream baffle to the baffle-shell boundary of the downstream baffle. Average Nusselt numbers in the eddy-flow zone are in general somewhat higher than in other zones while those in the cross-flow zone are in general lower. A wider range of flow rates must be studied to determine the effect of flow rate on average Nusselt numbers in each zone. The present results indicate that the average Nusselt numbers for each zone vary about as the six-tenths power of the flow rate. Baffle spacing may also have an effect here. The high value shown for the eddy flow zone at 120 cfm, 6 baffle case, could conceivably be due to extensive turbulence in the flowing fluid. There were indications that more choatic flow existed in the eddy zone for the six baffle case than the eddy zone for the ten baffle case.

TABLE 3

Average Nusselt Numbers in the Various Flow Zones

Number of Baffles	Rate of Flow cfm	Average Nusselt Numbers: Longitudinal Flow Zone	Cross-Flow Zone	Eddy Zone	Percent Increase in Eddy Zone over Cross Flow Zone	Overall Nusselt Number Nu_{oa}
6	58.65	75.82	70.07	77.83	11.11	72.80
6	90.39	98.90	89.12	98.44	10.50	95.04
6	119.30	118.48	110.41	140.91	27.60	123.62
10	58.73	86.75	92.56	93.83	1.37	91.36
10	90.38	110.49	110.51	118.02	6.80	113.18
10	117.60	131.39	129.55	144.32	11.40	135.36

Conclusions:

Local heat-transfer coefficients have been determined at 3/4-in. intervals between the central two segmental baffles of a tubular heat exchanger. Two baffle spacings and three flow rates were studied.

Overall Nusselt numbers calculated from the measured local coefficients agree favorably with values of overall Nusselt numbers obtained by Williams and Katz (7) on tubular heat exchangers. Local coefficients obtained in the present work agree with those obtained by Ambrose (1) on the same apparatus.

Heat-transfer coefficients are high in the baffle hole, decrease rapidly along the length of the tube and midway between the two baffles reach a minimum value which is one-fourth to one-half of the value at the baffle hole.

The actual effect of tube-to-baffle clearance cannot be determined until knowledge of the amount of leakage through the clearance is obtained.

The results indicate the presence of three flow zones in the baffle space.

The average Nusselt number for the eddy-flow zone being in general higher than that in either the cross-flow or longitudinal-flow zones. Fluid motion appears more choatic in the eddy-flow zone for the six baffle case than for the ten baffle case.

Acknowledgment:

Appreciation is expressed to the National Science Foundation for a grant to support this research project.

REFERENCES

1. Ambrose, T. W., Ph.D. Thesis, Oregon State College (1957)
2. Ambrose, T. W. and J. G. Knudsen, Local Shell-Side Heat Transfer Coefficients in Baffled Tubular Heat Exchangers, paper presented at the Annual Meeting of the A.I.Ch.E., Chicago, Illinois, December 8-12, 1957.
3. Giedt, W. H., Trans. A.S.M.E., 71, 375 (1949)
4. Gupta, Rajeshesar K. and Donald L. Katz, Ind. Eng. Chem., 49, 998 (1957)
5. Gurushankariah, Mysore S., M.S. thesis, Oregon State College (1958)
6. Milne, William E., "Numerical Calculus", p. 96, Princeton University Press (1949)
7. Williams, R. B. and D. L. Katz, Trans. A.S.M.E., 74: 1307 (1952).

NOMENCLATURE

A Area, ft.^{2}; A_c Cross-flow area in tube tank at shell diameter; A_w is baffle window free area

C_p Specific heat at a constant pressure Btu/(lb)(^oF)

d Diameter of tube, ft.

G_e Weighted mass velocity, lbs/(hr)(ft^2) = $\dfrac{W}{\sqrt{A_w A_c}}$

h Local heat transfer coefficient, Btu/(hr)(ft^2)(^oF)

h_{av} Average heat transfer coefficient around a tube

i Current, amperes

k Thermal conductivity, Btu/(hr)(ft^2)(^oF)/ft.

q_{cond} Heat conducted into plastic tube, Btu/hr.

q_{rad} Heat radiated from ribbons Btu/hr.

R Resistance of ribbon

r Radius, ft.

s Baffle spacing, ft.

t Temperature, ^oF; t_a, air temperature ^oF

W Width of resistance ribbon, ft.

w Mass flow rate, lbs/hr.

Z Thickness of resistance ribbon, ft.

θ Angle measured from leading edge of a tube, degrees

μ Viscosity of air, lb /(ft^2)(hr)

Nu_{av} $h_{av}h/k$, average Nusselt number at a position around a tube, Nu_c, average Nusselt number at a cross-section in the heat exchanger, Nu_{od} average overall Nusselt number in a baffle space

Pr Prandtl number

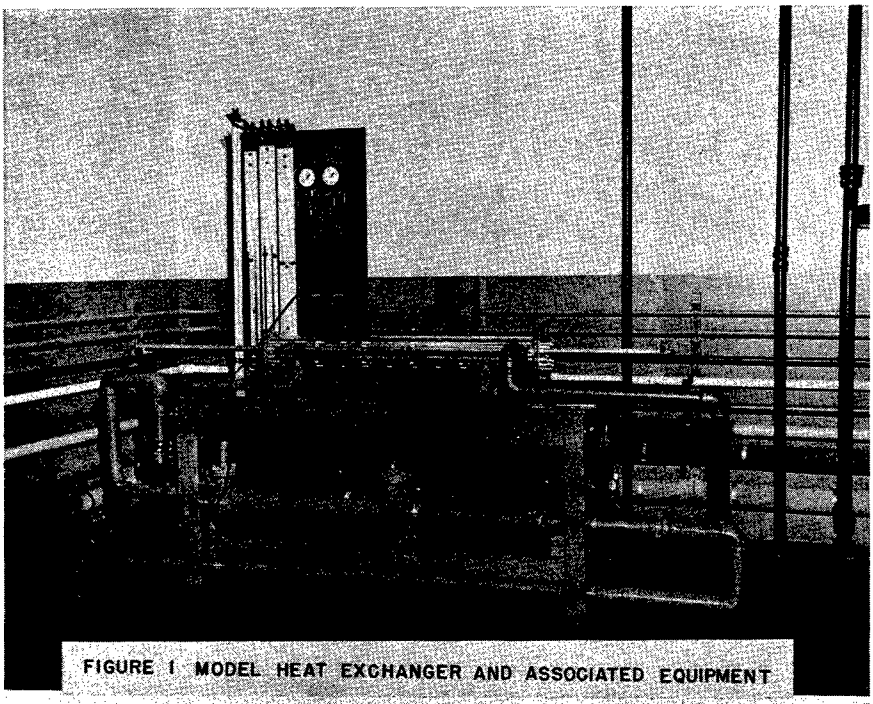

FIGURE 1 MODEL HEAT EXCHANGER AND ASSOCIATED EQUIPMENT

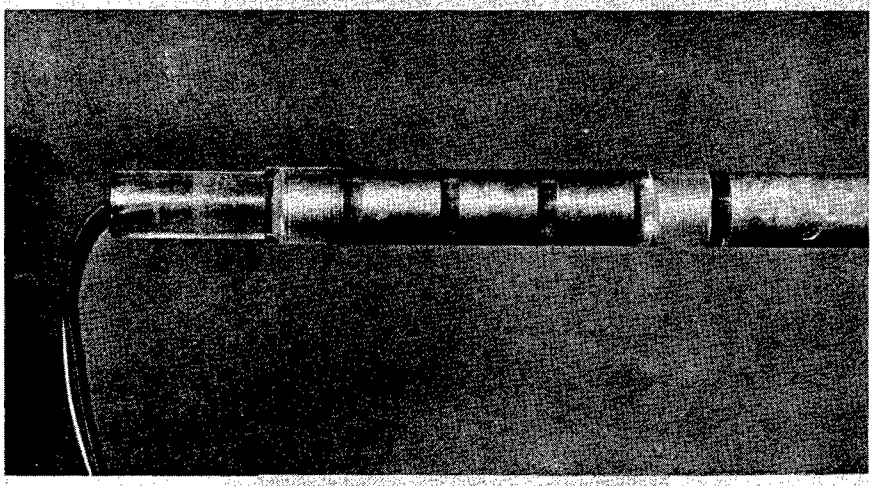

FIGURE 2 SENSING PROBE

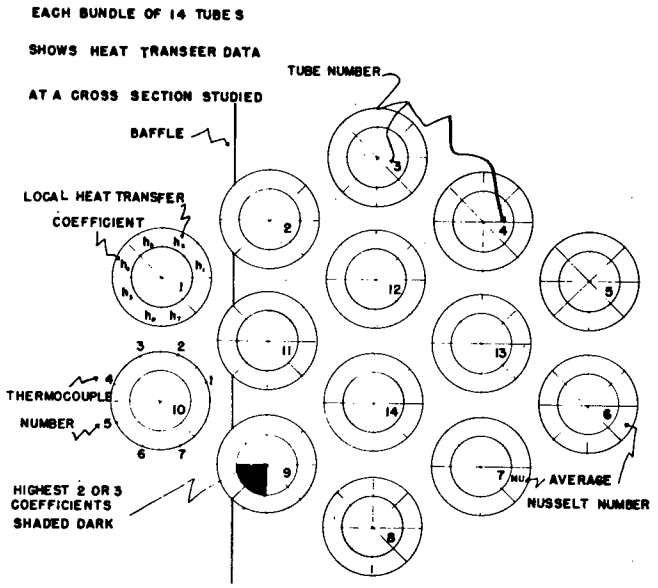

GRAPHICAL PRESENTATION SYSTEM OF HEAT TRANSFER DATA
FIGURE 3

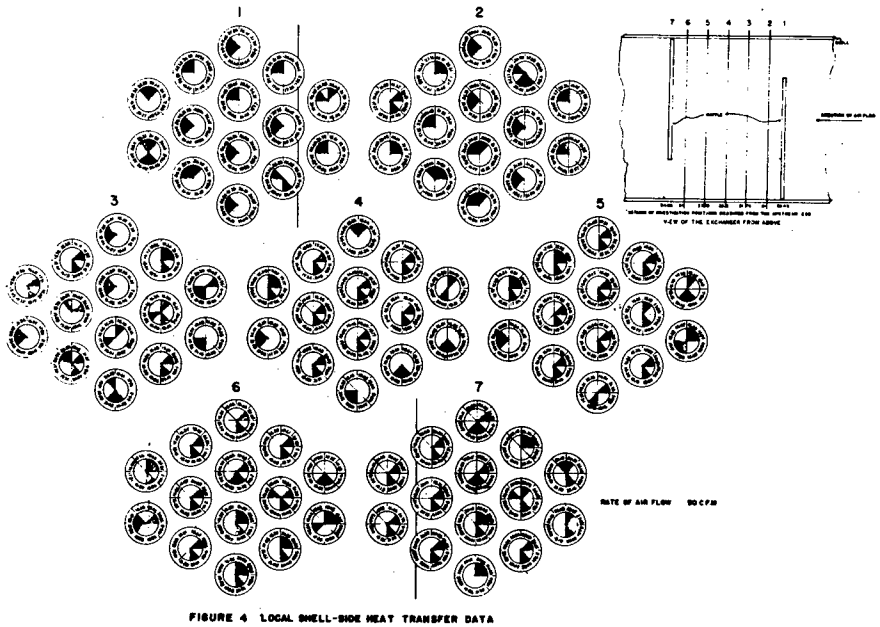

FIGURE 4 LOCAL SHELL-SIDE HEAT TRANSFER DATA

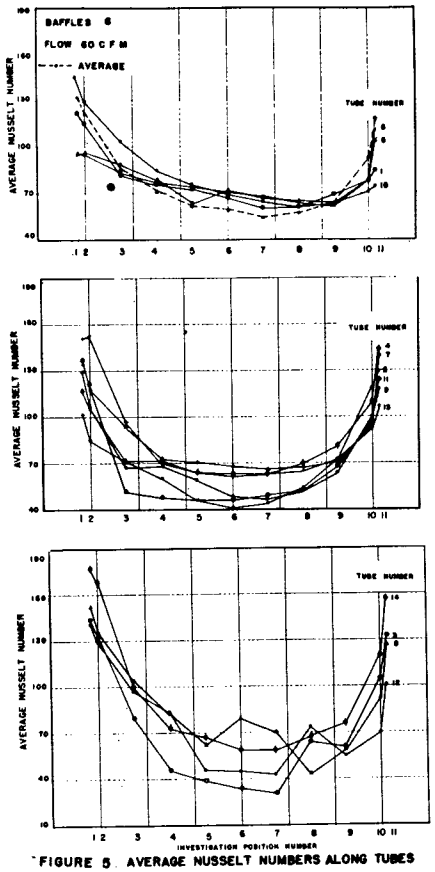

FIGURE 5 AVERAGE NUSSELT NUMBERS ALONG TUBES

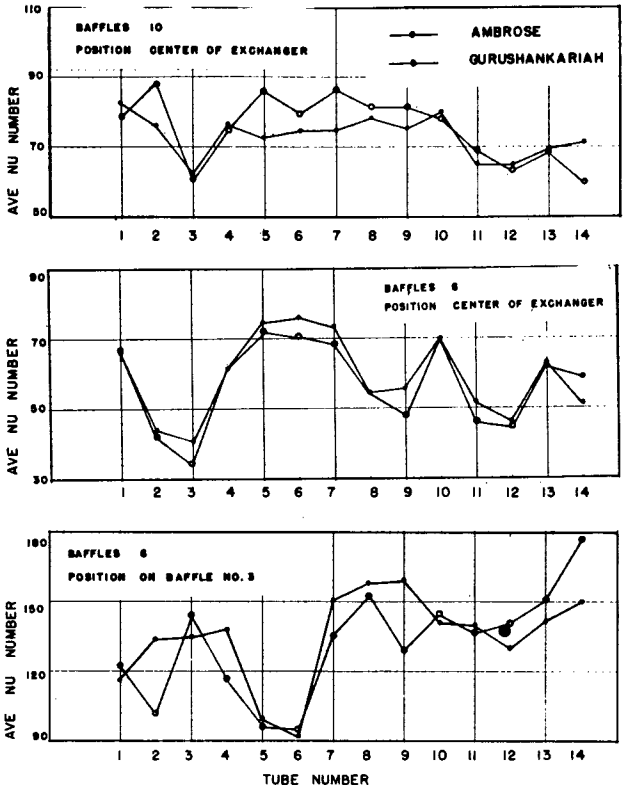

FIGURE 8 COMPARISON OF AVERAGE NUSSELT NUMBERS WITH MEASUREMENTS MADE BY AMBROSE

19-24
26

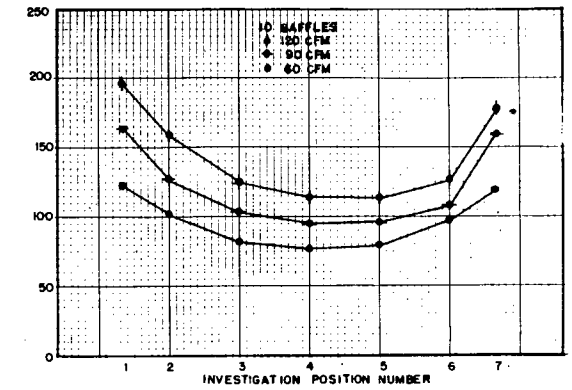

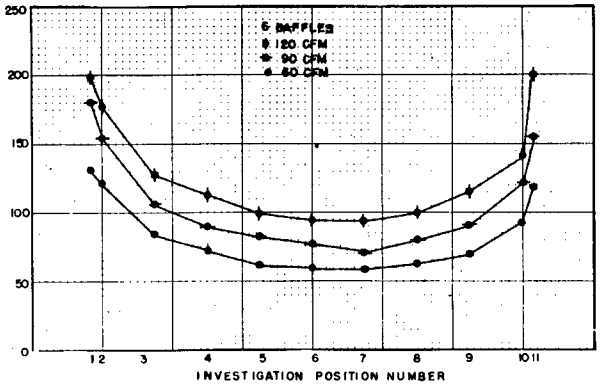

FIGURE 6 AVERAGE NUSSELT NUMBERS AT A CROSS SECTION

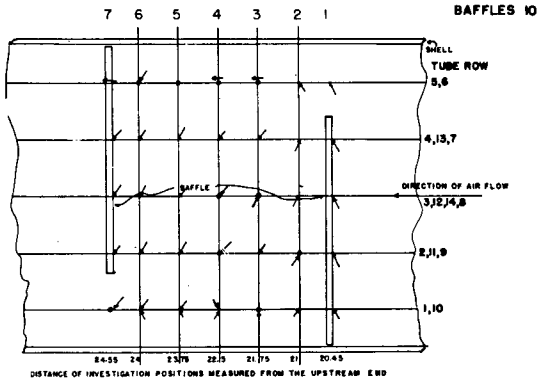

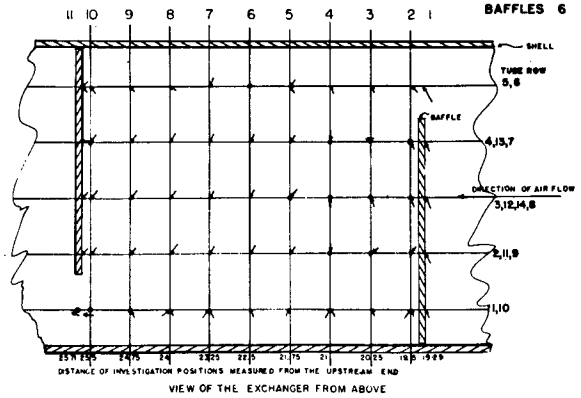

FIGURE 9 SCHEMATIC DIAGRAM OF THE FLOW PATTERN

19-39
36

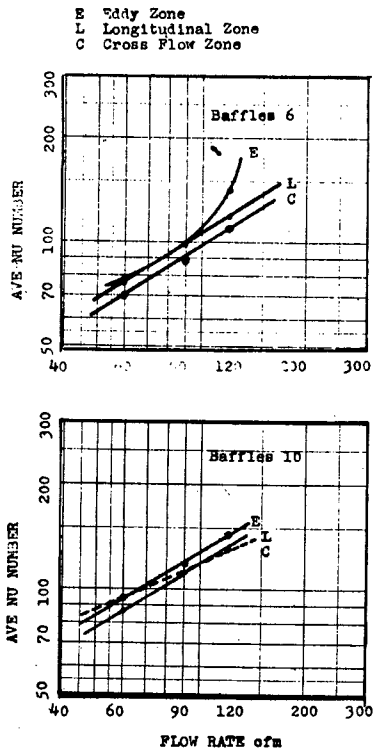

FIGURE 10 VARIATION OF NUSSELT NUMBERS WITH FLOW RATE

A GURUSHANKARIAH (6" SHELL, 1" TUBES, 1 1/4" TUBE PITCH)

B AMBROSE -do-

C WILLIAMS AND KATZ (6" SHELL, 3/8" TUBES, 1/2" TUBE PITCH)

D WILLIAMS AND KATZ (8" SHELL, 1/2" TUBES, 5/8" TUBE PITCH)

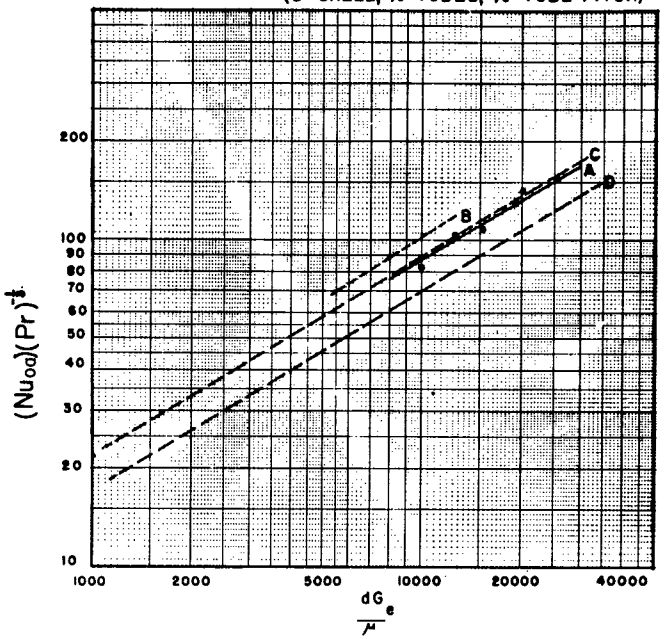

CORRELATION OF SHELL-SIDE HEAT TRANSFER DATA

FIGURE 7